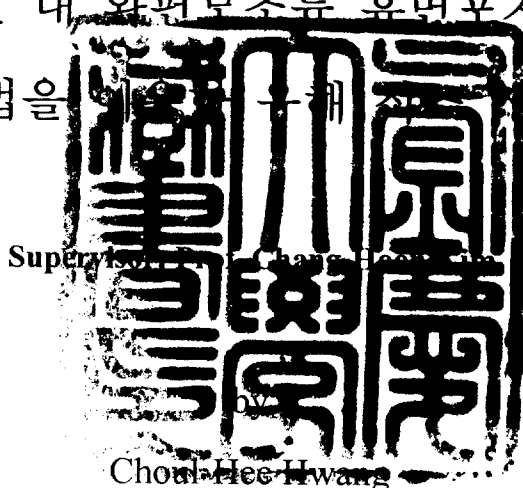


Spatial Distribution of Dinoflagellate Resting Cysts and Detection of HAB species using PCR assay in Sediments of the Yellow Sea

황해 저질 내 와편모조류 휴면포자 분포와
PCR 기법을 이용한 유해 조류 검출



A thesis submitted in partial fulfillment of the requirements
for the degree of Master of Science
in Department of Fisheries Biology, Graduate School,
Pukyong National University
February 2006

황철희의 수산학석사 학위논문을 인준함

2006년 2월 일

주 심

이학박사

남 윤 권



위 원

이학박사

김 종 명



위 원

농학박사

김 창 훈



Spatial Distribution of Dinoflagellate Resting Cysts and Detection of HAB species using PCR assay in Sediments of the Yellow Sea

A Dissertation

By

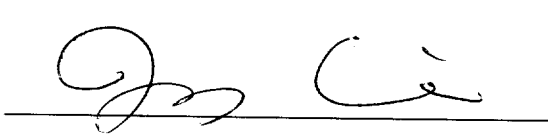
Choul-Hee Hwang

Approved as to style and content by

A handwritten signature in black ink, appearing to read 'YK Nam', written over a horizontal line.

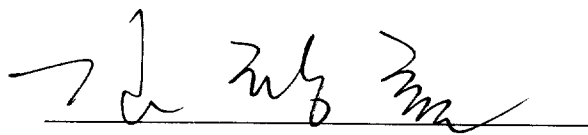
Dr. Yoon Kwon Nam

Chairman

A handwritten signature in black ink, appearing to read 'JMK', written over a horizontal line.

Dr. Jong-Myung Kim

Member

A handwritten signature in black ink, appearing to read 'CHK', written over a horizontal line.

Dr. Chang-Hoon Kim

Member

February 28, 2006

Contents

Abstract	2
Figure legends	4
Table legends.....	6
1. Introduction	7
2. Material and Methods	
2-1. Sediment sampling satations	10
2-2. Treatment of sediment samples.....	12
2-3. Bulk-DNA extraction of sediment samples from the Yellow Sea	14
2-4. PCR amplification.....	14
3. Results	
3-1. Identification.....	16
3-2. A tendency of distribution	17
3-3. PCR amplification using yellow soil.	26
3-4. Detection of <i>Alexandrium tamarense</i> and <i>Cochlodinium polykrikoides</i>	28
4. Discussion	31
References	36
Summary (in Korean).....	43
Acknowledgements	45

Spatial Distribution of Dinoflagellate Resting Cysts and Detection of HAB species using PCR assay in Sediments of the Yellow Sea

Choul-Hee Hwang

Department of Fisheries Biology, Graduate School,
Pukyong National University
Busan 608-737, Korea

Abstract

The spatial distribution of dinoflagellate resting cysts in sediment samples of the Yellow Sea has been studied through the analysis of 33 samples by the palynological process. The sampling areas comprised four latitudinal transects, the northernmost of which was located off the Shandong Peninsula, China and the southernmost off Jeju Island, Korea. Each transect line was composed of six to nine stations, spanning between the Chinese and Korean coasts. A total of 26 different types of dinoflagellate resting cysts were identified. *Gonyaulax scrippsae*, *Alexandrium* spp. (ellipsoidal type) and *Gonyaulax spinifera* were dominant at all stations surveyed. The latitudinal distribution trend showed that resting cyst concentrations were much higher along the inner two transects than those along the outer two transects. For each transect, resting cyst concentrations reached the highest in the offshore central areas and gradually decreased nearer to the Chinese and Korean coasts. This concentric resting cyst distribution pattern was correlated with hydrographic features such as circular current systems, sedimentary properties and water depth of the Yellow Sea.

Outbreaks of harmful dinoflagellate blooms of *Alexandrium tamarense* and *Cochlodinium polykrikoides* have gradually increased in Korea coastal waters and caused severe damage to mariculture industry. In order to detect and monitor these harmful dinoflagellates in sediment samples, the PCR detection assay was adopted. This technique was applied to extracted bulk DNA from the Yellow Sea. The PCR amplification using *A. tamarense*-specific primer pairs did not yield any visible products for yellow soil (a negative control), but produced clear bands successfully after ellipsoidal *Alexandrium* cysts were

artificially added. Thus, yellow soil seemed to be an excellent negative control, not including genomic DNA of a targeted organism. In the Yellow Sea sediments samples, *A. tamarense* and *C. polykrikoides* were detected, species-specific primer pairs being used by the PCR assay. On the other hand, as it was hard to assess the concentration of resting cysts in the sediment by the detection assay, nested PCR was adopted to identify the definite existence of *C. polykrikoides*. Therefore, the PCR detection assay is expected to be used on the basis of molecular biological detection assays for the HAB monitoring and identification of harmful species such as *C. polykrikoides*, whose life cycle is not explained.

Figure legends

- Fig. 1. Sampling stations of sediment samples established in this study.
- Fig. 2. Analytical processes of dinoflagellate resting cysts in sediment samples using Cho and Matsuoka (2001) method.
- Fig. 3. The contour map of the spatial distribution of the total dinoflagellate cysts in the Yellow Sea. Contour lines are increments of 1,000 cells g⁻¹ dry weight.
- Fig. 4. Longitudinal change in relative abundance of dinoflagellate cysts in each transect categorized by motile cell-based classification in the Yellow Sea.
- Fig. 5. The contour map of the spatial distribution of ellipsoidal *Alexandrium* spp. resting cyst in the Yellow Sea. Contour lines are increments of 1,000 cells g⁻¹ dry weight.
- Fig. 6. Photomicrographs of dinoflagellate resting cysts investigated in this study after palynological process; 1) *Alexandrium* spp. (ellipsoidal type), 2) *Alexandrium* spp. (ovoidal type), 3-4) *Gonyaulax scrippsae*, 5) *G. verior*, 6) *G. spinifera* complex, 7) *Scrippsiella trochoidea*, 8) *Protoperidinium* spp., 9) *Protoperidinium* spp. (spherical), 10-11) *Lingulodinium polyedrum*, 12) *Protoceratium reticulatum*, 13) *Pyrodinium bahamense* var. *compressum*, 14-15) *Pheopolykrikos hartmannii*, 16) unidentified, 17) *Pyrophacus steinii*, 18) *Protoperidinium latissimum*, 19) *Protoperidinium* sp. and 20) *P. oblongum*
- Fig. 7. The detection of *Alexandrium tamarense* using *A. tamarense*-specific primer pairs in yellow soil from the Mt. Hwang-lyeng Lane designations are as follows: M= 250bp size marker; 1= yellow soil; 2= yellow soil-ellipsoidal *Alexandrium* resting cyst 10cells; 3= yellow soil-ellipsoidal *Alexandrium* resting cyst 50cells; 4= sediment sample from the Yellow Sea; *A. tamarense* culture sample (KDD8); 6= Negative control.
- Fig. 8. The detection of *Alexandrium tamarense* using *A. tamarense* species-specific primer pairs in sediment samples from the Yellow Sea using *A. tamarense* species-specific primer pairs. Lane designations are as follows: M= 250bp size marker; 1= A2; 2= A3; 3= A4; 4= B4; 5= B5; 6= B6; 7= C4; 8= C5; 9= C6; 10= D4; 11= D5; 12= D6; 13= *A. tamarense* culture sample; 14= yellow soil.
- Fig. 9. The detection of *Cochlodinium polykrikoides* in sediment samples from the Yellow

Sea using the *C. polykrikoides* species-specific primer pairs, CPOLY01 and CPOLY02. Lane designations are as follows: M= 250bp size marker; 1= A2; 2= A3; 3= A4; 4= B4; 5= B5; 6= B6; 7= C4; 8= C5; 9= C6; 10= D4; 11= D5; 12= D6; 13= *C. polykrikoides* culture sample; 14= yellow soil.

Table legends

- Table 1. The latitude / longitude and water depth of each station investigated in the Yellow Sea
- Table 2. Distribution of dinoflagellate cysts (cells g⁻¹ dry weight) in the surface sediments of transect A in the Yellow Sea
- Table 3. Distribution of dinoflagellate cysts (cells g⁻¹ dry weight) in the surface sediments of transect B in the Yellow Sea
- Table 4. Distribution of dinoflagellate cysts (cells g⁻¹ dry weight) in the surface sediments of transect C in the Yellow Sea
- Table 5. Distribution of dinoflagellate cysts (cells g⁻¹ dry weight) in the surface sediments of transect D in the Yellow Sea

Spatial Distribution of Dinoflagellate Resting Cysts and Detection of HAB species using PCR assay in Sediments of the Yellow Sea

1. Introduction

The Yellow Sea, which was investigated in this study, forms one of the largest epicontinental shelves. It is partially enclosed by the Chinese and Korean coasts and borders on the Bohai Sea and the East China Sea. It rests in a tectonically stable trough that was submerged during the postglacial sea-level rise, with an average water depth of 55 m (Jin and Chough, 1998; Uehara and Saito, 2003).

The general hydrographic features of the Yellow Sea are characterized by the northward inflow of the Yellow Sea Warm Current and the subsequent southward flows along the Chinese and Korean coasts (i.e. the Yellow Sea Coastal Current and the Korean Coastal Current). These coastal currents are compensated by the northward flow of the Yellow Sea Cold Bottom Water along the Yellow Sea trough, which forms the big cyclonic (counterclockwise) eddy in the central part of the Yellow Sea, which has a relatively weak hydrodynamic condition (Naimie et al., 2001 Shi et al., 2004).

Sediments of the Yellow Sea consist of sand, muddy sand, sandy mud and mud, ordered by the percentage of mud or sand. The suspended fine-grained materials nearshore move along the route of the Yellow Sea circulation mentioned above, and are transported to and accumulated on the seafloor at the eddy center of the Yellow Sea to form the muddy sediments. As a result, the largest mud-rich sediment patch is developed in the central part of the Yellow Sea, and muddy sand and sand are distributed outward (Park and Khim, 1992; Uehara and Saito, 2003; Shi et al., 2004).

The harmful algal bloom (HAB) is a worldwide problem in the marine environment such as related to economic loss and toxin production in last decades (Kim, 1997). The main HAB-causative organisms composed of diatoms until the 1970s have been replaced by flagellates since the early 1980s in Korea (Chang et al. 1995; Kim et al. 1997; Lee 1999).

The main HAB species in Korea were *Alexandrium* spp., *Gymnodinium* spp., *Prorocentrum* spp. and *Cochlodinium polykrikoides*. Specially, *Alexandrium* spp. are notorious as producers of paralytic shellfish toxin (PSP; Kim, 1997) and *C. polykrikoides* also produces of ichthyotoxin and sometimes results in mass fish mortality through suffocation by oxygen depletion and mucus production (Lee, 1996; Cho et al., 1999; Kim et al., 2000). They often have detrimental effects on marine animals followed by huge economic loss to local fisheries and mariculture industries.

PSP contamination has annually caused the ban on shellfish harvesting, and continuous PSP monitoring has been conducted around shellfish-farming areas worldwide. Two PSP accidents, which resulted in human deaths, occurred in China (Kin-Chung, 1998) and Korea (Chang et al., 1987; Lee et al., 1997). The main causative microorganisms were *Alexandrium catenella*, *A. tamarense* and *Gymnodinium catenatum* (Han et al., 1992; Kim and Shin, 1997; Kin-Chung, 1998; Park et al., 2004b). Meanwhile, shellfish mariculture has developed rapidly on the eastern coast of China over the last two decades (Guo et al., 1999), and shellfish intoxication by various algal toxins has been concomitantly reported (Anderson et al., 1996; Zhou et al., 1999). Jeon et al. (1988) reported PSP contamination on the western coast of Korea. The resting cysts of the causative dinoflagellates (e.g. *A. tamarense/catenella* and *G. catenatum*) are ubiquitously present in the sediments of the Yellow Sea (Cho and Matsuoka, 2001; Park et al., 2004a, b; Wang et al., 2004). Since then, the governmental institute has conducted continuous PSP monitoring and has temporarily inhibited mussel harvesting when the toxin content exceeds the quarantine level of 80 µg STXeq 100g⁻¹.

Cochlodinium polykrikoides blooms which have been notorious for high cell density, high fish mortality, long persistency, wide spreading and increasing frequency since 1982 caused the record-breaking economic loss of US \$ 95.5 million in 1995 (Kim et al., 1997). Therefore, the primary strategy for managing the effects of these blooms in a monitoring program aimed that its early detection. However, some organisms such as *C. polykrikoides* were difficult to forecast its early outbreak because of the unclear life cycle.

HABs have been the subject of many researchers because of their increasing outbreak, extension and protraction (Hallegraeff, 1993). A number of dinoflagellates cause HABs in

the marine ecosystem. Some of them have complex life cycles that include benthic cyst stages. Dinoflagellate resting cysts play important ecological roles such as bloom initiation and termination, agents of survival and dispersal, genetic recombination, and potential toxin source of benthic mollusks. Geographical resting cyst mapping thus pinpoints the presence of "seed populations" for bloom initiation sites and traces dispersal paths that suggest the potential for future HAB outbreaks and are useful for HAB controls (Dale, 1983; Anderson, 1984; Pfister and Anderson, 1987).

The first step to HAB monitoring was rapid and accurate identification and numeration of the causative organism. However, recognizing morphological characteristics under light microscopy consume much time and effort, and require sophisticated expertise. Moreover, the conventional monitoring of *C. polykrikoides* is seriously hampered by distortion of the cell morphology that occurs after fixation. Lee et al., (2001) reported that *C. polykrikoides* was indistinguishably similar with *Gymnodinium catenatum*, *G. impudicum*. To overcome such problems, molecular techniques such as PCR assay, fluorescence *in situ* hybridization (FISH), Sandwich-hybridization and immunological assay have recently been developed (Scholin et al., 2003). The nuclear-encoded large subunit ribosomal DNA (LSU rDNA) molecules that contain both conserved and divergent domains have been used to resolve identification and phylogenetic relationships of dinoflagellates in wide taxonomic levels (Scholin et al., 1994; Zardoya et al., 1995; Daugbjerg et al., 2000; Rehnstam-Holm et al., 2002; Edvardsen et al., 2003).

As part of the HAB monitoring, marine sediment samples of the Yellow Sea were investigated for spatial distribution, species composition and molecular detection of dinoflagellate resting cysts. The resting cyst distribution was compared to hydrographic and sedimentary properties of the Yellow Sea to understand their origin, dispersal path and depositional site. Moreover, existence of target HAB species (*A. tamarensis* and *C. polykrikoides*) was analyzed using species-specific primer pairs targeting the LSU rDNA D1-D3 region by bulk DNA from sediment samples.

2. Material and Methods

2-1. Stations of sediment sample

A cruise for this study was conducted around the Yellow Sea (Fig. 1, Table 1) on 15-31 October 2003 using the *R/V Tamgu 8* of the West Sea Fisheries Research Institute, National Fisheries Research and Development Institute (NFRDI), Korea. Sediment samples were collected with a Van Veen grab sampler from 33 stations on four transect lines that ran latitudinally between the Chinese and Korean coasts. Transect A was the northernmost transect and was located off the Shandong Peninsula and Transect D was the southernmost and was located off Jeju Island. Transects B and C were located central of the Yellow Sea.

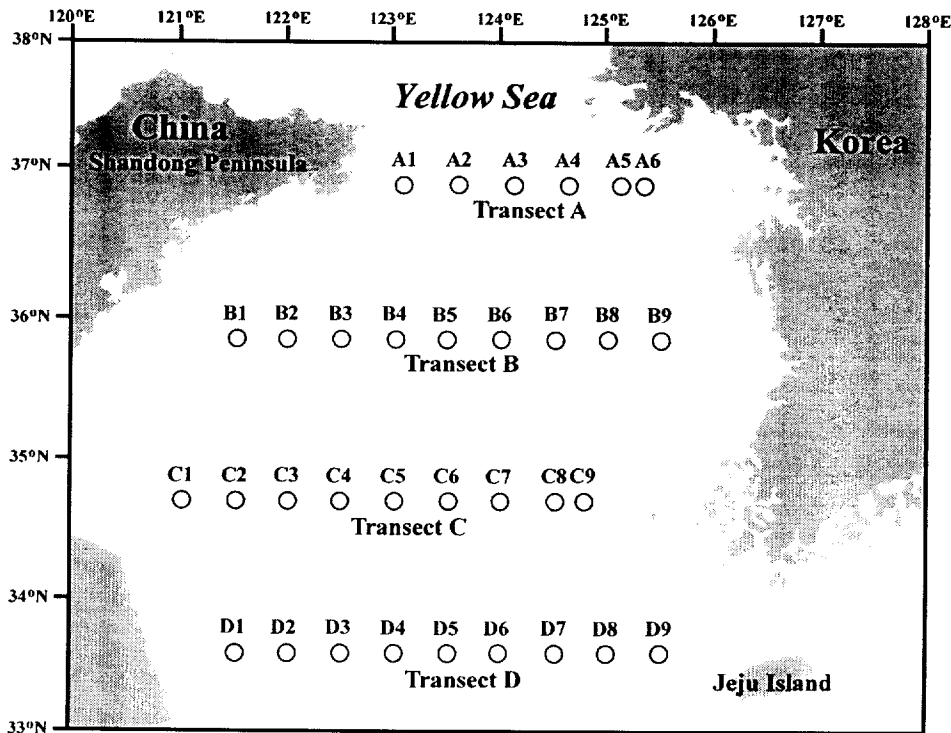


Fig. 1. Sampling stations of sediment samples investigated in this study.

Table 1. The latitude / longitude and water depth of each station investigated in the Yellow Sea

Station	Latitude (N)	Longitude (E)	Water depth (m)
Transect A			
A1	36°55'50"	123°07'70"	47
A2	36°55'50"	123°37'70"	75
A3	36°55'50"	124°07'70"	77
A4	36°55'50"	124°37'70"	78
A5	36°55'50"	125°07'70"	50
A6	36°55'50"	125°20'70"	55
Transect B			
B1	35°51'30"	121°32'00"	40
B2	35°51'30"	122°02'00"	46
B3	35°51'30"	122°32'00"	61
B4	35°51'30"	123°02'00"	70
B5	35°51'30"	123°32'00"	73
B6	35°51'30"	124°02'00"	77
B7	35°51'30"	124°32'00"	85
B8	35°51'30"	125°02'00"	77
B9	35°51'30"	125°32'00"	71
Transect C			
C1	34°43'00"	121°02'00"	25
C2	34°43'00"	121°32'00"	43
C3	34°43'00"	122°02'00"	50
C4	34°43'00"	122°32'00"	66
C5	34°43'00"	123°02'00"	75
C6	34°43'00"	123°32'00"	78
C7	34°43'00"	124°02'00"	80
C8	34°43'00"	124°32'00"	93
C9	34°43'00"	124°49'00"	87
Transect D			
D1	33°34'70"	121°32'00"	20
D2	33°34'70"	122°02'00"	26
D3	33°34'70"	122°32'00"	41
D4	33°34'70"	123°02'00"	49
D5	33°34'70"	123°32'00"	67
D6	33°34'70"	124°02'00"	73
D7	33°34'70"	124°32'00"	84
D8	33°34'70"	125°02'00"	85
D9	33°34'70"	125°32'00"	90

2-2. Treatment of sediment samples

Sediment samples were collected with a Van Veen grab sampler from 33 stations on four transect lines that ran latitudinally between the Chinese and Korean coasts. The northernmost transect was located off the Shandong Peninsula of China, and the southernmost transect off Jeju Island of Korea, in a longitudinal direction. The top surface fractions of grab samples were carefully collected and pooled on board the ship, and the stored at 4°C in the dark until analysis.

After calculating water contents, sediment samples were processed according to Cho and Matsuoka (2001). The samples were first treated with 10% hydrochloric acid (HCl) and 47% hydrofluoric acid (HF) to dissolve calcium carbonate and silicate materials, respectively. Subsequently they were rinsed with distilled water, and sonicated using an Ultrasonic Cleaner 5210 (BRANSON) for 30 sec. After straining through 120 µm and 20 µm mesh sieves, the refined sediments remaining on the 20 µm sieve were transferred to a 15 mL tube and finally suspended into 10 mL of distilled water. A 1 mL aliquot of each sample was observed under an inverted light microscope (Axiovert 200 ZEISS, Germany). Cyst concentrations were calculated as the number of cysts per gram of dry weight.

Identification was carried out according to Matsuoka and Fukuyo (2000). In this study, resting cysts are called as cysts for the sake of brevity. Only living cysts were counted.

1) Measuring water contents

- ← Weight the triplicate sediments
- ← Dry at oven (60°C for overnight)

2) Cyst analysis

- ← 10% HCl: dissolving calcium carbonate
(foraminiferal, molluscan and other calcareous fragments)
- ← Washing
- ← 47% HF: dissolving silicate materials
(sand and mud particles or diatom frustules)
- ← Washing
- ← Sonication
- ← Fraction

Observation

Fig. 2. Analytical processes of dinoflagellate resting cysts in sediment samples.

2-3. Bulk-DNA extraction from sediment samples

The sediments samples of the central area of the Yellow Sea used to detect of target organisms because cyst densities were higher than other areas, and then stored at -70°C in the dark until analysis. One ml of denaturation solution [10 mM Tris-HCl (pH 7.0), 1 mM EDTA and 0.5% 2-mercaptoethanol] and 2 g of sea sand were added in 2 g sediment samples. These samples were completely pulverized in liquid nitrogen. These pulverized sediments were put in a 50 ml centrifuge tube, and extraction buffer [100 mM sodium phosphate (pH 7.0), 100 mM Tris-HCl (pH 7.0), 100 mM EDTA (pH 8.0), 1.5 M NaCl, 1% CTAB, 2% SDS] was added. Bulk DNA was extracted at 65°C for 1 hour (Hurt et al., 2001). The extracted bulk DNA was separated by PCI solution (Phenol: Chloroform: Isoamyl alcohol; 3-Methylbutanol 25:24:1), and precipitated by ethanol. The DNA sample was purified by QIAEX II Agarose Gel Extraction Kit (QIAGEN) to remove humic acid and others mineral materials. Culture cells of *A. tamarense* and *C. polykrikoides* were used as positive controls to tune target organisms, and bulk DNA from yellow soil from Mt. Hwang-lyeng was used as a negative control.

the total DNA contents were confirmed by electrophoresis in 1% agarose gel in TAE buffer (40 mM Tris/acetate, 1 mM EDTA) at 100mV for 20min and photographed under UV trans-illumination after staining with EtBr (0.5 $\mu\text{g mL}^{-1}$).

2-4. PCR amplification

PCR amplification was carried out in a 50 μL -reaction volume containing 0.25 units *Ex Taq*TM (TaKaRa, Japan), 1 \times *Ex Taq*TM Buffer, 2.5 mM of each dNTP, species-specific primer pairs and 1 μL of template DNA. A PCR reaction was one initial denaturation at 94°C for 3 min, followed by 25 cycles of denaturation at 94°C for 30 sec, annealing at 58°C for 1 min and elongation at 72°C for 1 min. The reaction was completed by the final elongation at 72°C for 7 min (My Cycler, Bio-Rad). PCR products (5 μL) were electrophoresed in 1% agarose gel in TAE buffer (40 mM Tris / acetate, 1 mM EDTA) at 100 mV for 20 min and photographed under UV trans-illumination after staining with EtBr (0.5 $\mu\text{g mL}^{-1}$)

The species-specific primer pairs used to detection *A. tamarense* were Atama-L416F (TTG

CTT GGT GGG AGT GTT GCA) and D3B (5'-TCG GAA GGA ACC AGC TAC TA-3'; Nunn et al., 1996). Nested PCR was carried out to detect *C. polykrikoides* (Sharrocks, 1994). For the nested PCR assay, the primary PCR was first carried out with an universal primer set, D1R (5'-ACC CGC TGA ATT TAA GCA TA-3'; Scholin et al., 1994) and D3B (5'-TCG GAA GGA ACC AGC TAC TA-3' ; Nunn et al., 1996), followed by the secondary PCR with specific primer pairs such as CPOLY01 (5'-GTA CAC GGC TTG CAC TTG CA-3') and CPOLY02 (5'-TGG TCG TAG ACG TGT GTC AG-3'; Kim et al., 2004a).

3. Results

3-1. Identification

In this study, a total of 26 different types of dinoflagellate cysts were identified to the species level, representing 15 genera and belonging to the orders Gonyaulacales (11 species), Peridiniales (10 species) and Gymnodiniales (5 species) (Tables 2, 3, 4 and 5). The most common species were *Gonyaulax scrippsae*, *Alexandrium* spp. (ellipsoidal type) and *G. spinifera*, all of which belong to the Gonyaulacales. Concentrations of *Protoceratium reticulatum*, *G. verior* and *Scrippsiella trochoidea* were also relatively high. Other types of cysts occurred in relatively low numbers.

Transect A was the northernmost transect and was located off the Shandong Peninsula. At transect A, 24 types of cysts were identified (Table 2). Cyst concentrations were significantly higher at Stns A1-A4 (3,180-5,398 cells g⁻¹ dry weight) in the central areas of transect than at Stns A5 and A6 in the marginal areas of the Korean coast (Fig. 3). *Alexandrium* spp. (ellipsoidal type 96-2,153 cells g⁻¹) were the most abundant, followed by *G. scrippsae* (9-844 cells g⁻¹), *G. spinifera* (6-489 cells g⁻¹), *G. verior* (18-319 cells g⁻¹), *P. reticulatum* (6-443 cells g⁻¹) and *Pheopolykrikos hartmannii* (31-446 cells g⁻¹).

Twenty-four types of cysts were recorded from Transect B located south of Transect A (Table 3). Total concentrations were markedly high in the central areas (Stns B3-B6) (10,550-20,329 cells g⁻¹) and sharply decreased towards the coastal areas of China and Korea (Fig. 3). Stn B4 in the central region had the highest density of cysts (20,829 cells g⁻¹) of among all sediment samples analyzed. The major species identified were *G. scrippsae* (10-6,985 cells g⁻¹), *G. spinifera* (5-4,929 cells g⁻¹), *Alexandrium* spp. (ellipsoidal type 95-2,629 cells g⁻¹) and *P. reticulatum* (25-1,977 cells g⁻¹).

At Transect C located between Transect B and the southernmost Transect D, 24 types of cysts were encountered (Table 4). Cyst concentrations were high in the central areas (Stns C4-C6 12,106-18,873 cells g⁻¹) and sharply decreased towards the marginal areas of both the Chinese and Korean coasts. The lowest density among all sediment samples analyzed was recorded at Stn C1 on the Chinese coast (111 cells g⁻¹). The highest value was 18,873 cells g⁻¹ at Stn C6, where *Alexandrium* spp. (ellipsoidal type; 10,699 cells g⁻¹) contributed >50%

of the total concentration. The variation in the number of ellipsoidal *Alexandrium* cysts accounted for the substantial fluctuations in the total cyst concentrations. For example, the relatively low cyst concentration at Stn C5 was accompanied by the substantially low number of ellipsoidal *Alexandrium* cysts.

Transect D was the southernmost and was located off Jeju Island, identified a total of 23 cyst types (Table 5), and the inner stations showed much higher cyst concentrations (Stns D4-D6 4,035-5,979 cells g⁻¹) than did the outer stations (Fig. 3). The most dominant species was *G. scrippsae* (45-2,872 cells g⁻¹).

3-2. A tendency of distribution

On the whole, within each transect, cyst densities were highest near the offshore center of the Yellow Sea and gradually decreased towards both the Chinese and Korean coasts (Fig. 3). The inner Transects B and C showed higher concentrations than did the outer Transects A and D. However, the trend of gradual decrease towards the higher and lower latitudes was less prominent than that towards both near shore directions. Cyst concentrations on the Chinese coast were relatively lower than that on the Korean coast.

In general, dinoflagellate cysts belonging to the Gonyaulacales comprised over 50% of all cysts collected, and two exceptions of the abrupt proportional decrease of the Gonyaulacales at Stns C1 and D1 on the Chinese coast were noteworthy (Fig. 4). The proportional density of the Protoperidinales tended to gradually increase towards both the Chinese and Korean coasts, while total cyst concentrations dramatically decreased.

Table 2. Distribution of dinoflagellate cysts (cells g⁻¹ dry weight) in the surface sediments of transect A in the Yellow Sea

Species	Station	A1	A2	A3	A4	A5	A6
Gonyaulacales							
<i>Alexandrium</i> spp. (ellipsoidal)		578	716	2,153	1,730	96	344
<i>Alexandrium</i> spp. (spherical)		191	283	167	187	28	50
<i>Gonyaulax scrippsae</i>		404	407	844	219	9	33
<i>Gonyaulax spinifera</i>		431	318	489	160	6	40
<i>Gonyaulax verior</i>		117	142	319	261	18	53
<i>Lingulodinium polyedrum</i>		116	40	192	105	28	-
<i>Protoceratium reticulatum</i>		409	443	423	183	6	30
<i>Pyrodinium bahamense</i> var. <i>compressum</i>		82	48	27	32	6	20
<i>Pyrophacus steinii</i>		10	-	8	2	-	-
Gymnodiniales							
<i>Cochlodinium</i> sp.		5	7	8	-	4	4
<i>Gymnodinium catenatum</i>		147	31	55	30	9	-
<i>Gymnodinium impudicum</i>		54	5	13	-	1	-
<i>Pheopolykrikos hartmannii</i>		236	161	446	144	31	53
<i>Polykrikos kofoidii</i> /schwartzii		15	-	-	-	-	-
Peridinales							
<i>Diplopetta parva</i>		13	-	-	1	-	-
<i>Diplopsalis lenticula</i>		50	41	13	11	6	3
<i>Preperidinium meunieri</i>		8	3	6	3	-	-
<i>Protoperidinium conicum</i>		17	23	11	7	3	7
<i>Protoperidinium latisinum</i>		17	16	17	-	-	-
<i>Protoperidinium oblongum</i>		-	2	6	3	-	-
<i>Protoperidinium pentagonum</i>		-	-	-	3	-	-
<i>Protoperidinium</i> sp. (spherical)		32	33	68	72	-	-
<i>Protoperidinium</i> spp.		141	77	17	8	-	-
<i>Scripsiella trochoidea</i>		37	20	57	1	6	37
Unidentified		79	41	57	18	20	16
Total		3,188	2,857	5,398	3,180	277	693

Table 3. Distribution of dinoflagellate cysts (cells g⁻¹ dry weight) in the surface sediments of transect B in the Yellow Sea

Species	Station	B1	B2	B3	B4	B5	B6	B7	B8	B9
Gonyaulacales										
<i>Alexandrium</i> spp. (ellipsoidal)		95	126	500	2,408	2,629	541	530	1,876	287
<i>Alexandrium</i> spp. (ovoidal)		33	-	-	-	-	-	15	-	-
<i>Alexandrium</i> spp. (spherical)		243	154	468	375	542	109	65	185	15
<i>Gonyaulax scrippsae</i>		52	297	2,858	6,985	6,650	5,008	1,684	1,109	10
<i>Gonyaulax spinifera</i>		33	66	1,691	4,929	3,031	2,942	1,082	126	5
<i>Gonyaulax spinifera</i> complex		10	22	64	375	335	96	116	50	-
<i>Gonyaulax verior</i>		252	148	540	1,245	1,091	109	131	252	30
<i>Lingulodinium polyedrum</i>		29	66	564	300	508	68	116	126	-
<i>Protoceratium reticulatum</i>		252	472	1,977	1,336	1,465	1,840	1,488	433	25
<i>Pyrodinium bahamense</i> var. <i>compressum</i>		14	38	167	158	67	322	152	45	5
<i>Pyrophacus steinii</i>		-	-	16	-	-	-	-	-	-
Gymnodiniales										
<i>Cochlodinium</i> sp.		10	-	-	-	-	-	-	-	-
<i>Gymnodinium catenatum</i>		29	-	103	135	161	89	152	-	-
<i>Gymnodinium impudicum</i>		19	-	151	300	94	34	-	63	-
<i>Pheopolykrikos hartmannii</i>		105	121	294	330	529	445	254	1,087	-
Peridiniales										
<i>Diplopelta parva</i>		-	-	79	-	20	82	15	-	-
<i>Diplopsalis lenticula</i>		24	11	24	38	33	62	58	36	5
<i>Preperidinium meunieri</i>		-	-	-	30	27	-	15	-	-
<i>Protoperidinium conicum</i>		-	-	-	90	27	41	-	-	-
<i>Protoperidinium latisinum</i>		5	-	-	-	-	-	-	-	-
<i>Protoperidinium oblongum</i>		-	-	175	120	13	-	-	-	-
<i>Protoperidinium</i> sp. (spherical)		10	-	111	45	107	-	131	104	5
<i>Protoperidinium</i> spp.		148	176	119	391	161	151	94	95	25
<i>Scrippsiella trochoidea</i>		105	126	603	1,223	1,050	486	806	153	35
Unidentified		24	33	48	15	13	55	44	27	15
Total		1,489	1,856	10,550	20,829	18,553	12,479	6,947	5,767	462

Table 4. Distribution of dinoflagellate cysts (cells g⁻¹ dry weight) in the surface sediments of transect C in the Yellow Sea

Species	Station	C1	C2	C3	C4	C5	C6	C7	C8	C9
Gonyaulacales										
<i>Alexandrium</i> spp. (ellipsoidal)		5	65	128	5,656	1,030	10,699	41	194	855
<i>Alexandrium</i> spp. (ovoidal)		-	-	4	-	-	-	-	-	-
<i>Alexandrium</i> spp. (spherical)		23	70	71	463	9	726	-	-	70
<i>Gonyaulax scrippsae</i>		14	135	287	4,567	5,716	1,869	2,309	1,246	495
<i>Gonyaulax spinifera</i>		-	19	190	1,228	2,272	1,243	662	315	102
<i>Gonyaulax spinifera</i> complex		-	5	26	88	160	60	55	27	27
<i>Gonyaulax verior</i>		5	47	31	2,714	293	1,760	-	60	118
<i>Lingulodinium polyedrum</i>		-	33	9	250	80	159	62	20	5
<i>Protoceratium reticulatum</i>		-	135	379	750	257	577	1,082	395	543
<i>Pyrodinium bahamense</i> var. <i>compressum</i>		-	5	31	88	124	179	76	67	38
<i>Pyrophacus steinii</i>		-	5	4	-	-	40	-	-	-
Gymnodiniales										
<i>Cochlodinium</i> sp.		5	-	-	-	-	-	-	-	-
<i>Gymnodinium catenatum</i>		-	9	4	15	53	60	14	13	5
<i>Gymnodinium impudicum</i>		9	5	35	-	-	-	-	-	-
<i>Pheopolykrikos hartmannii</i>		14	28	13	338	44	328	248	167	317
<i>Polykrikos kofoidii</i> /schwartzii		1	-	-	-	-	-	-	-	-
Peridinales										
<i>Diplopelta parva</i>		-	-	-	-	27	-	7	-	5
<i>Diplopsalis lenticula</i>		-	9	18	15	107	119	138	54	5
<i>Preperidinium meunieri</i>		5	-	-	-	-	20	28	-	5
<i>Protoperidinium conicum</i>		-	9	18	22	-	10	-	13	-
<i>Protoperidinium oblongum</i>		5	5	-	29	18	20	14	-	-
<i>Protoperidinium</i> sp. (spherical)		-	9	9	74	44	159	28	13	5
<i>Protoperidinium</i> spp.		23	103	67	74	18	70	117	127	70
<i>Scrippsiella trochoidea</i>		-	9	93	699	1,784	696	283	87	70
Unidentified		5	9	18	22	71	80	28	27	16
Total		111	714	1,434	17,092	12,106	18,873	5,190	2,827	2,753

Table 5. Distribution of dinoflagellate cysts (cells g⁻¹ dry weight) in the surface sediments of transect D in the Yellow Sea

Species	Station	D1	D2	D3	D4	D5	D6	D7	D8	D9
Gonyaulacales										
<i>Alexandrium</i> spp. (ellipsoidal)		-	-	178	300	398	1,138	199	193	109
<i>Alexandrium</i> spp. (ovoidal)		-	-	7	19	-	-	19	5	6
<i>Alexandrium</i> spp. (spherical)		110	10	36	138	509	206	12	27	19
<i>Gonyaulax scrippsae</i>		46	45	721	2,063	1,305	2,872	1,207	529	410
<i>Gonyaulax spinifera</i>		37	30	336	544	731	845	224	182	237
<i>Gonyaulax spinifera</i> complex		18	15	-	50	56	29	37	16	6
<i>Gonyaulax verior</i>		83	-	50	169	93	51	87	96	26
<i>Lingulodinium polyedrum</i>		18	-	21	156	46	73	-	16	6
<i>Protoceratium reticulatum</i>		-	30	178	288	185	81	100	96	103
<i>Pyrodinium bahamense</i> var. <i>compressum</i>		-	-	29	106	9	22	6	-	-
<i>Pyrophacus steinii</i>		-	-	7	-	-	-	25	5	6
Gymnodiniales										
<i>Cochlodinium</i> sp.		64	-	-	-	-	-	-	5	-
<i>Gymnodinium catenatum</i>		18	-	29	-	130	73	-	11	6
<i>Gymnodinium impudicum</i>		-	10	7	25	28	29	19	16	26
<i>Pheopolykrikos hartmannii</i>		120	5	79	269	185	235	75	59	26
<i>Polykrikos kofoidii/schwartzii</i>		55	5	-	-	9	-	6	-	6
Peridinales										
<i>Diplopelta parva</i>		-	-	14	-	19	22	-	-	-
<i>Diplopsalis lenticula</i>		9	-	7	6	-	44	31	11	32
<i>Protoperidinium conicum</i>		9	-	7	13	9	22	19	21	-
<i>Protoperidinium oblongum</i>		-	-	-	-	9	-	12	-	-
<i>Protoperidinium</i> sp. (spherical)		9	20	7	13	65	29	31	16	-
<i>Protoperidinium</i> spp.		82	25	28	76	93	22	56	80	12
<i>Scrippsiella trochoidea</i>		28	5	71	125	111	125	37	21	96
Unidentified		9	10	14	6	46	59	6	-	6
Total		717	210	1,827	4,364	4,035	5,979	2,208	1,406	1,141

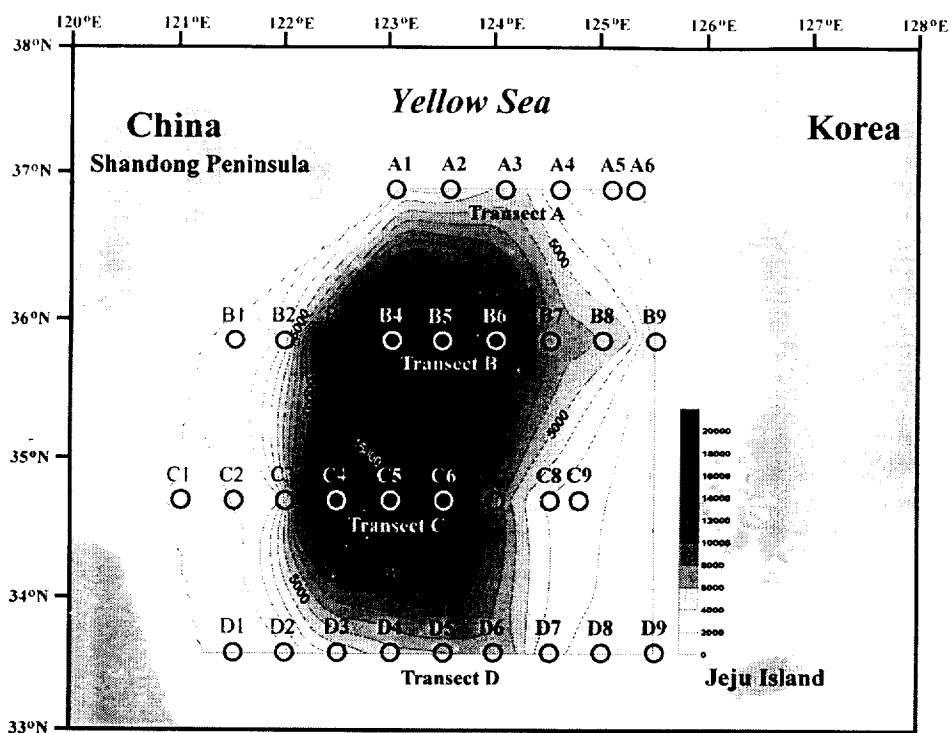


Fig.3. The contour map of the spatial distribution of the total dinoflagellate cysts in the Yellow Sea. Contour lines are increments of 1,000 cells g⁻¹ dry weight.

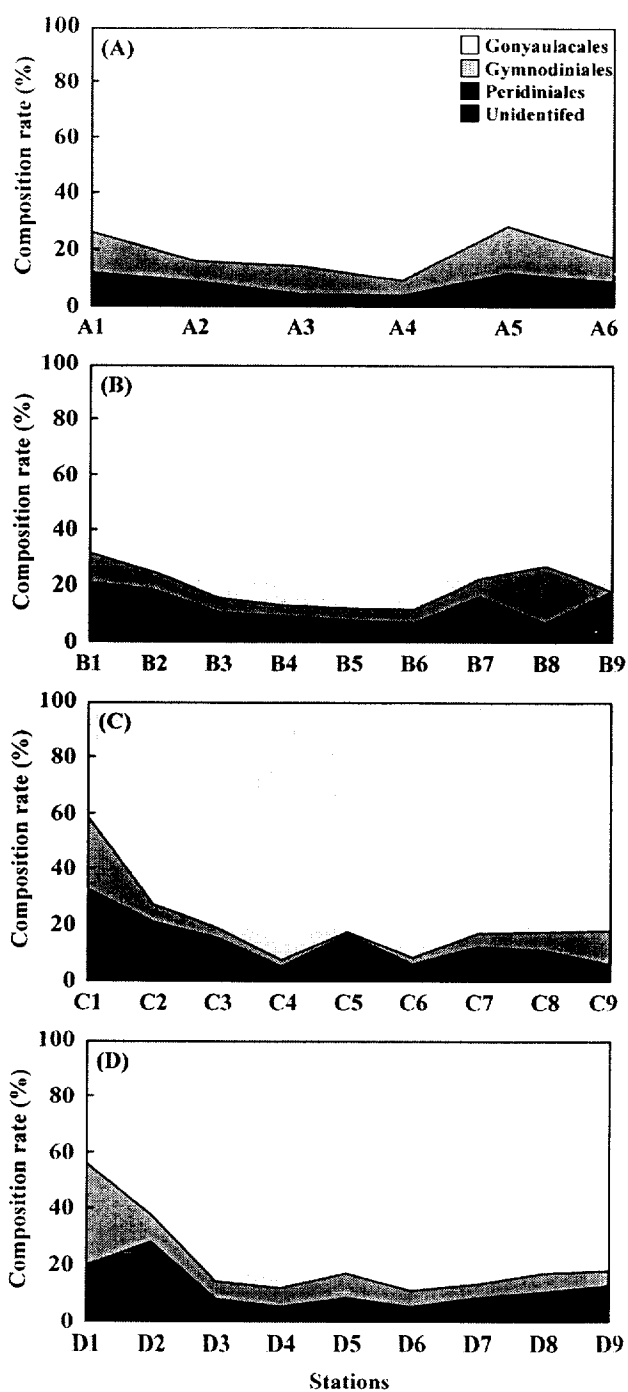


Fig. 4. Longitudinal change in relative abundance of dinoflagellate cysts in each transect categorized by motile cell-based classification in the Yellow Sea.

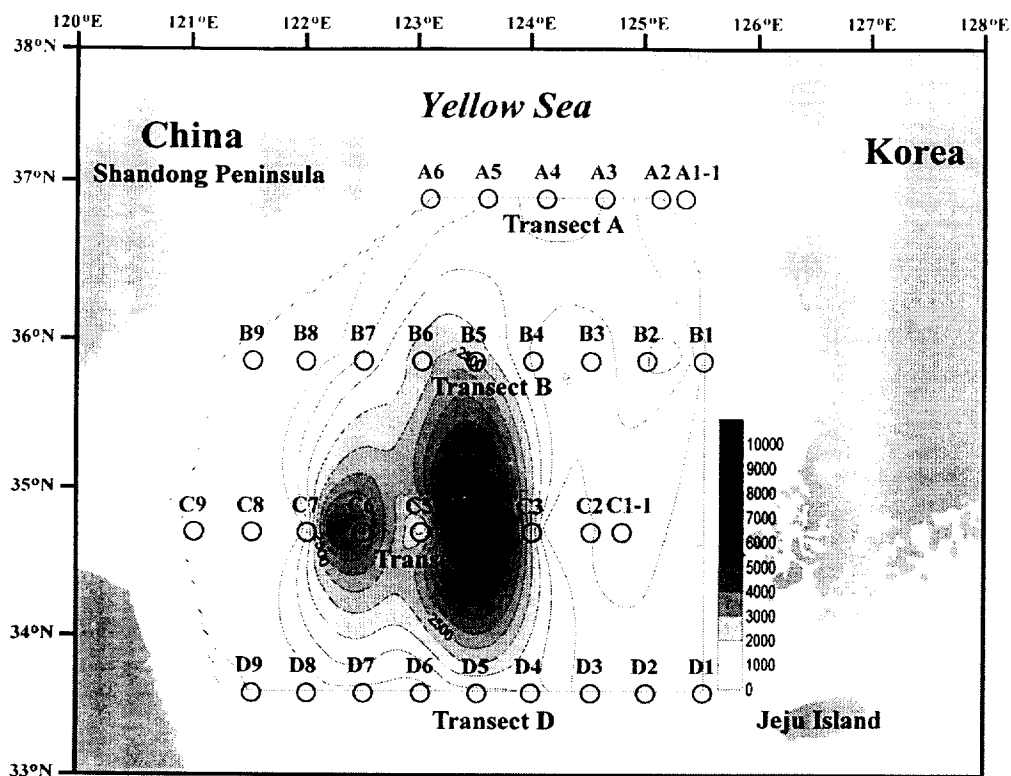


Fig. 5. The contour map of the spatial distribution of ellipsoidal *Alexandrium* spp. resting cyst in the Yellow Sea. Contour lines are increments of 1,000 cells g⁻¹ dry weight.

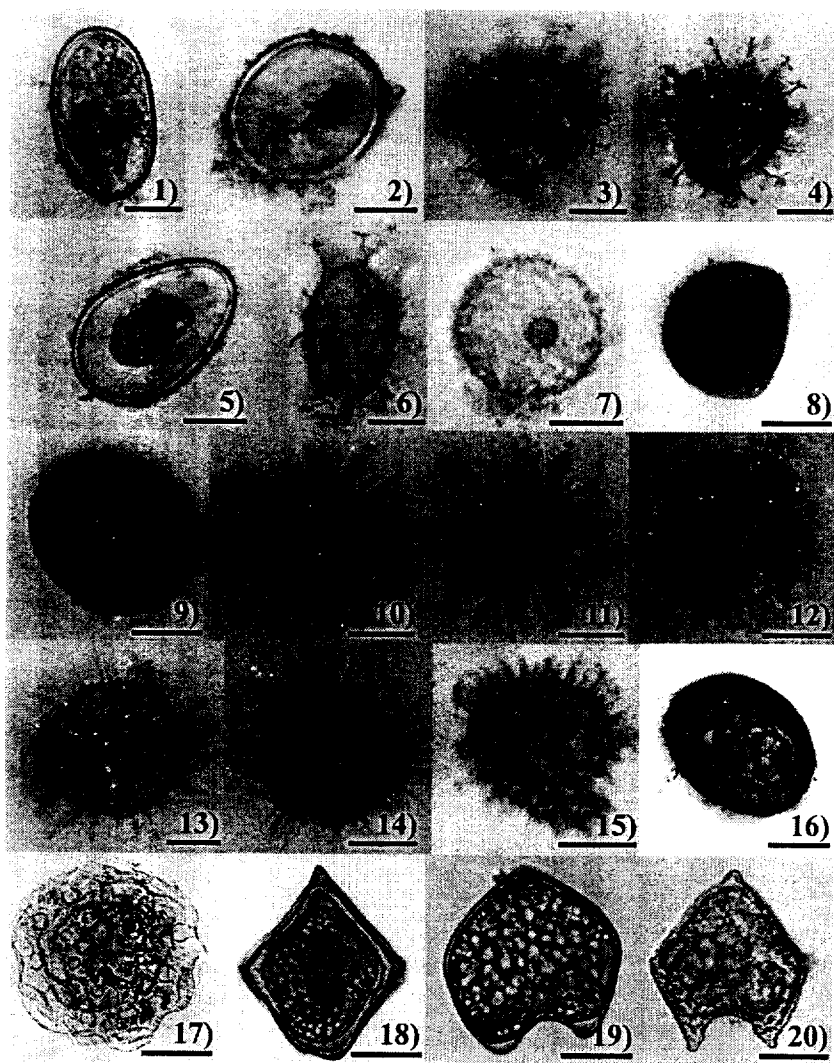


Fig. 6. Photomicrographs of dinoflagellate resting cysts investigated in this study after palynological process (scale bar is 100 μm) ; 1) *Alexandrium* spp. (ellipsoidal type), 2) *Alexandrium* spp. (ovoidal type), 3-4) *Gonyaulax scrippsae*, 5) *G. verior*, 6) *G. spinifera* complex, 7) *Scrippsiella trochoidea*, 8) *Protoperidinium* spp., 9) *Protoperidinium* spp. (spherical), 10-11) *Lingulodinium polyedrum*, 12) *Protoceratium reticulatum*, 13) *Pyrodinium bahamense* var. *compressum*, 14-15) *Pheopolykrikos hartmannii*, 16) unidentified, 17) *Pyrophacus steinii*, 18) *Protoperidinium latissimum*, 19) *Protoperidinium* sp. and 20) *P. oblongum*

3-3. PCR amplification

There were no amplifications in yellow soil collected from Mt. Hwang-lyeng using *A. tamarense* species-specific primer pairs. However, a positive control, in which ellipsoidal *Alexandrium* cysts was added, was successfully amplified with a primer set, Atama-L416F and D3B. Furthermore, the sediment samples of the Yellow Sea containing a number of ellipsoidal *Alexandrium* cysts were successfully amplified (Fig. 7). Thus yellow soil collected from a mountain did not include *A. tamarense* resting cyst as expected, and can be used as a practical negative control for HAB monitoring. Also, the specificity of *A. tamarense*-specific primer pairs and usefulness of PCR detection assay for monitoring of target HAB species were demonstrated.

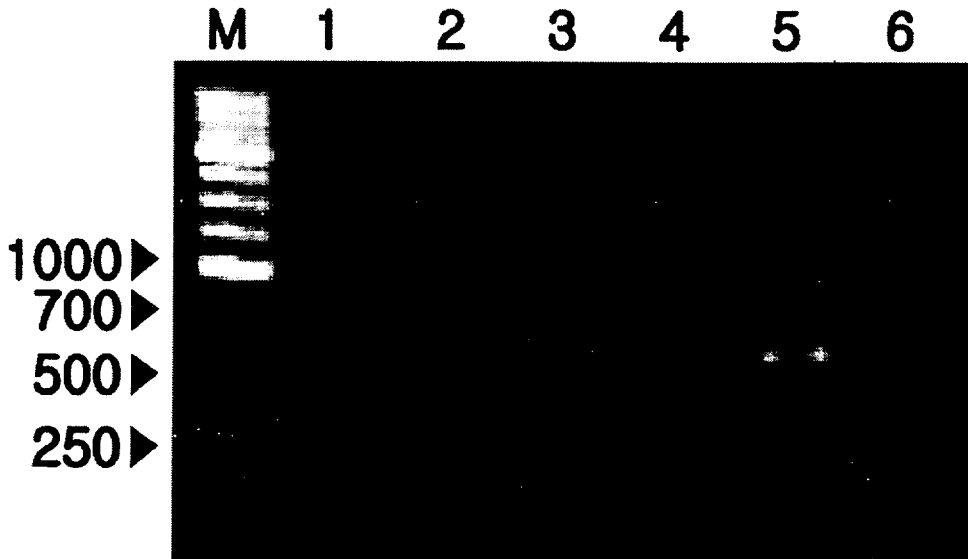


Fig. 7. The detection of *Alexandrium tamarense* using *A. tamarense*-specific primer pairs in yellow soil from the Mt. Hwang-lyeng. Lane designations are as follows: M = 250 bp size marker; 1 = yellow soil; 2 = yellow soil containing 10 cells of ellipsoidal *Alexandrium* resting cysts; 3 = yellow soil containing 50cells of ellipsoidal *Alexandrium* resting cysts; 4 = sediment sample from the Yellow Sea containing *A. tamarense* culture cells; 6= a negative control.

3-4. Detection of *Alexandrium tamarense* and *Cochlodinium polykrikoides*

Twelve sediment samples were selected from central areas in the Yellow Sea based on concentrations of ellipsoidal *Alexandrium* cysts. The LSU rDNA region was PCR-amplified by *A. tamarense*-specific primer pairs (Fig. 8). The PCR amplification of 13 samples including a positive control yielded only one predicted fragment of > 500 base pair (bp). This result is exactly the same with those of identification by palynological process.

A primer pair, D1R and D3B was first used to amplify environmental bulk DNAs to detect *C. polykrikoides* at Stns A2, A3, A4, B4, B5, and D6 (Fig. 9). The PCR products were subsequently amplified by *C. polykrikoides*-specific primer pair. The PCR amplification yielded only one predicted fragment of < 500 bp. Therefore, the resting cysts of two species could be detected by PCR amplification in the sediment samples, and PCR assays were highly specific and sensitive.

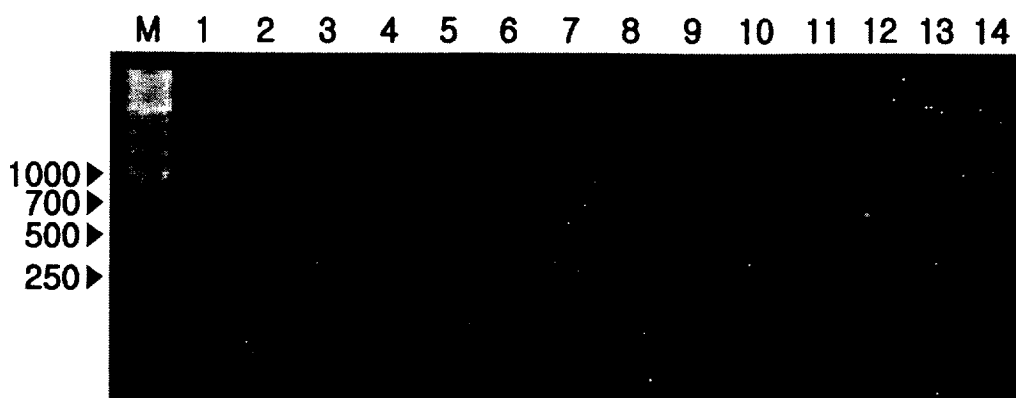


Fig. 8. The detection of *Alexandrium tamarense* in sediment samples from the Yellow Sea using the *A. tamarense*-specific primer pair. Lane designations are as follows: M = 250 bp size marker; 1 = A2; 2 = A3; 3 = A4; 4 = B4; 5 = B5; 6 = B6; 7 = C4; 8 = C5; 9 = C6; 10 = D4; 11 = D5; 12 = D6; 13 = *A. tamarense* culture sample (a positive control); 14 = yellow soil (a negative control).

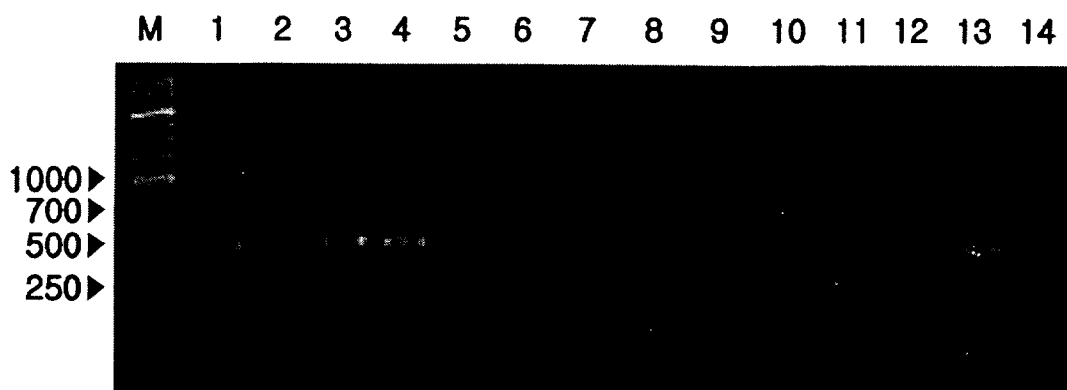


Fig. 9. The detection of *Cochlodinium polykrikoides* in sediment samples from the Yellow Sea using the *C. polykrikoides*-specific primer pairs, CPOLY01 and CPOLY02. Lane designations are as follows: M = 250 bp size marker; 1 = A2; 2 = A3; 3 = A4; 4 = B4; 5 = B5; 6 = B6; 7 = C4; 8 = C5; 9 = C6; 10 = D4; 11 = D5; 12 = D6; 13 = *C. polykrikoides* culture sample (a positive control); 14= yellow soil (a negative control).

4. Discussion

The 33 sediment samples surveyed in this study provided dinoflagellate cyst records from nearly the entire Yellow Sea continental shelf. Previously, Cho and Matsuoka (2001) investigated the spatial distributions of cysts in the East China Sea and the Yellow Sea. They noted unusually high cyst concentrations in the offshore center of the Yellow Sea, which was congruent with our results. However, their study areas covered only partial areas, and thus provided limited information on the biogeography of dinoflagellate cysts.

The sampling stations surveyed in this study covered wide areas along four latitudinal transects that connected the Chinese and Korean coasts, of which the northernmost transect was level with the Shandon Peninsula and the southernmost with Jeju Island. Overall, cyst concentrations were markedly elevated around the center of the Yellow Sea and gradually decreased in all four outward directions. The results in the study, high offshore cyst concentrations in the Yellow Sea were comparable to those of Cho et al. (2003), who reported that the number of cysts at offshore stations was approximately four times higher than those at inshore stations in the southern Korea Sea. This tendency towards increased cyst abundance in an offshore direction has also been well documented in previous studies (e.g. Wall et al., 1977; White and Lewis, 1982; Cho and Matsuoka, 2001; Dale et al., 2002). The total number of cysts recorded around the offshore center of the Yellow Sea was much higher than those of previous studies from the Korean coast (Lee et al., 1998; Kim et al., 2003; Park and Yoon, 2003; Park et al., 2004a).

The distribution of dinoflagellate cysts is usually governed not only by environmental factors such as the particle size of sediment, sedimentation rate, and hydrographic and geographical features, but also by biological factors (Dale, 1976; Wall et al., 1977; White and Lewis, 1982; Harland, 1983; Goodman et al., 1987; Turgeon et al., 1990). Cysts behave as fine-grained sedimentary particles, and they move and concentrate along hydrodynamic systems by the winnowing effects of neritic suspended particles containing various microfloras and microfaunas.

The hydrographic features of the Yellow Sea are characterized by the large cyclonic eddy in the central Yellow Sea trough, which has a relatively weak hydrodynamic condition (Naimie et al., 2001; Shi et al., 2004). Sediment distributions are under the direct influence

of the centrifugal force of this current movement. As a result, the largest fine-grained muddy deposits are located in the offshore central Yellow Sea (Park and Khim, 1992; Uehara and Saito, 2003; Shi et al., 2004). Shi et al. (2004) demonstrated that the net transport direction of sediments in the Yellow Sea was toward the central fine-grained sediment deposits. This sediment transport pattern was also consistent with several tracers of sediment sources such as the distribution of total suspended matter (TSM) concentrations, the $\delta^{13}\text{C}$ value of particulate organic carbon (POC), values of polycyclic aromatic hydrocarbons (PHAs) (Shi et al., 2004), and various geochemical elements (Kim et al., 1998). These sedimentary materials were originated and dispersed from the old- and present-day Huanghe (Yellow River) system (Alexander et al., 1991; Park and Khim, 1992; Shi et al., 2004).

The results in this study showing the concentric high-density cyst concentrations in the Yellow Sea were also congruent with these sedimentary properties, which were strongly correlated with a bathymetric feature (e.g. water depth) and the circulation system of the current. Thus, the high cyst concentrations in the offshore central Yellow Sea can be attributed to the prevailing Yellow Sea circulation of the current system associated with the transportation and deposition of fine-grained sediments. A tendency for an increase in the relative abundance of cysts along a deep-sea gradient may be largely influenced by larger-scale offshore transport of neritic and estuarine cysts to deeper depositional sites (Wall et al., 1977; Goodman, 1987; Dale et al., 2002).

Besides the underlying possibility of the exogenous origin of most benthic cysts in the central Yellow Sea mentioned above, there are also possibilities for endogenous origins, e.g. offshore migration of neritic bloom populations or vertical sinking of *in situ* bloom populations from the overlying water column after sexual reproduction (Tyler et al., 1982; McGillicuddy et al., 2003). An endogenous origin was actually supported by the spring phytoplankton bloom in the central Yellow Sea (Hyun and Kim, 2003).

Several scientists have suggested that marine environmental conditions could be estimated by changes in total cyst productivity and proportional changes of a certain taxon (Versteegh, 1994; Sære et al., 1997; Dale et al., 1999, 2002; Matsuoka, 1999). For example, a high relative abundance of heterotrophic protoperidinioid cysts occurs in nutrient-enriched areas such as nutrient-enriched upwelling or eutrophicated coastal areas (Versteegh, 1994; Dale et al., 2002). The proportion of heterotrophic cysts belonging to the Protoperidinales

was lowest in the central Yellow Sea and gradually increased towards the Chinese and Korean coasts along with the dramatic decrease in the total cyst concentrations. The significant proportional increase of protoperidinioid cysts towards the Chinese coast is noteworthy, and may at least imply that environmental conditions in these coastal areas differ from conditions from at other areas. However, this interpretation may be arbitrary, due to transport and dispersal of sedimentary materials containing micro floras by the prevailing hydrographic system mentioned above.

Molecular detection of HAB species using specific-species primer pairs showed that PCR assays were very useful for the detection of *A. tamarens* and *C. polykrikoides* in sediment samples. The yellow soil collected from a mountain used as a negative control because of absence of dinoflagellate cysts. The PCR amplification using *A. tamarens*-specific primer pairs did not yield any visible products for yellow soil (a negative control), but successfully produced clear bands after ellipsoidal *Alexandrium* cysts were for artificially added. Thus yellow soil did not include genomic DNA of a targeted organism, and it seems that yellow soil is an excellent negative control.

Specific primers, Atm1 targeting *A. tamarens* and CPOLY01 and CPOLY02 targeting *C. polykrikoides* were previously demonstrated to be species-specific through PCR amplification using vegetative cells (Kim et al., 2004a). In this study resting cysts of the two species were detected by PCR assays in the sediment samples. Nested PCR for detection of *C. polykrikoides* was conducted because of low reactivity. Sensitivity of nested PCR has been demonstrated to be at least 10,000 times higher than direct PCR (Miserez et al., 1997). In the Yellow Sea sediments samples, *A. tamarens* and *C. polykrikoides* were detected using species-specific primer pairs by PCR assays. The results of PCR detection assays were coincident with those of palynological process. This result highly suggests the usefulness of PCR detection assay for HAB monitoring.

Molecular approaches using species-specific genetic markers hold precise and rapid species identification. PCR is a considerably cheap and easy method. However, PCR-based methods for detection purposes have no possibility that both find out shape of target cells and quantitative analysis because DNA of target cells was required for bulk DNA extraction. HAB monitoring using PCR assay is useful for fast information on the presence or absence

of a target species. For more accurate monitoring, the application of molecular techniques such as competitive PCR (Saito et al., 2002), real-time PCR (Bowers et al., 2000; Tengs et al., 2001), sandwich-hybridization (Scholin et al., 1997; Tyrrell et al., 2002) and fluorescence in situ hybridization (Miller and Scholin, 1996) will be required to detect and enumerate HAB species from field samples.

The results in this study indicated that the combination of conventional observation using optical microscope and molecular assay were very useful for HAB monitoring. The conventional microscopic observation based on the measurement of morphologic characters such as size, shape and so on, is time-consuming and requires considerable taxonomic experience (Godhe et al., 2001). PCR amplification using species-specific primer pairs with high sensitivity can overcome these problems in part. Bolch (2001) successfully disrupted cyst walls of *G. catenatum* and amplified desired fragments of single cysts isolated by a micropipette after exposing the cysts to repetitive rounds of liquid nitrogen and boiling temperature. The combination of micropipette isolation and PCR amplification requires careful processing in the isolation step. Therefore, the detection method from sediment by PCR amplification will help HAB monitoring and identification of unconfirmed resting cysts.

Ellipsoidal *Alexandrium* cysts composed of *A. acatenella*, *A. catenella*, *A. fundyense*, *A. tamarensense* and *A. tamiyavanichii* (Yoshida et al., 2003) were the most ubiquitous taxa recorded in the Yellow Sea. Some of these species can produce PSP toxins and frequently occur in the coastal waters of China and Korea (Han et al., 1993; Zhou et al., 1999; Kim et al., 2002). The geographic range of ellipsoidal *Alexandrium* cysts in the Yellow Sea was extensive with high concentric offshore accumulations, the values of which are comparable to those of other coastal areas (for references, see Cho and Matsuoka, 2001). Over the last two decades, southern coastal areas of Korea have suffered from annual PSP incidents in fall and spring, accompanied by great economic losses caused by the ban on shellfish harvesting (Kim, 1997). Jeon et al. (1988) reported actual shellfish contaminations by PSP on the western coast of Korea. Kim et al. (2002) established several PSP-causing *A. tamarensense* isolates from resting cysts in the sediment samples of the Yellow Sea, and Kim and Kim (2004) showed their extreme homogeneity of rDNA sequence data to other isolates from other coastal waters around Korea and other countries. Therefore, the offshore reservoir of

high benthic cyst concentrations may play a critical role in providing inoculum sites for rapid *Alexandrium* blooms of large quantities in the overlying water column under favorable growth conditions (White and Lewis, 1982; Turgeon et al., 1990; McGillicuddy et al., 2003). Thus there is great potential for future PSP outbreaks in coastal areas around the Yellow Sea, and this necessitates periodic and persistent HAB monitoring.

Cochlodinium polykrikoides has bloomed and spread every summer, causing great economic loss to fisheries industry (Kim, 1997). However, *C. polykrikoides* was difficult to identification of resting cyst because of incomplete knowledge of the life-cycle, and the lack of morphologically informative characters for unequivocal species identification (Lee et al., 2001). Suh et al. (2004) reported that HAB detection around Korean waters using satellite remote sensing for monitoring, and they indicated that *C. polykrikoides* blooming was closely related with the current, coastal upwelling of cold water, chlorophyll *a* variation and organic materials.

Among 2,000 extant dinoflagellate species, only ca. 5% of species are known to have the corresponding cyst stage in the life cycle (Matsuoka and Fukuyo, 2003). Cyst morphologies of many notorious HAB species such as *C. polykrikoides*, *Karenia brevis* and *K. mikimotoi* remain unknown, and this prohibits their geographical mapping, which would be useful for efficient HAB prediction and control. The recent accumulation of molecular sequence data of HAB species and the development of molecular techniques have enabled to design sensitive and accurate oligonucleotide probes, and to detect and even quantify the HAB species of interest (Kim et al., 2004a and references therein). Practically, various molecular detection assays have been applied to dinoflagellate cysts present in the marine sediments (e.g. Godhe et al., 2002; Saito et al., 2002). Therefore, it may be possible to draw biogeographical maps of previously unidentified taxa in sediment samples as long as appropriate DNA probes are available. Our ongoing study focuses on the application of such up-to-date molecular tools to the sediment samples of the Yellow Sea for the genetic profiling of HAB species for which geographical mapping has been impossible.

References

- Alexander, C. R., DeMaster, D. J. and Nittrouer, C. A. 1991. Sediment accumulation in a modern epicontinental-shelf setting: the Yellow Sea. *Mar. Geol.* 98: 51-72.
- Anderson, D. M. 1984. Shellfish toxicity and dormant cysts in toxic dinoflagellate blooms. In: *Seafood Toxins*, Ragelis, E. P. (ed.). American Chemical Society, Washington D.C. pp. 125-138.
- Anderson, D. M., Kulis, D. M., Qi, Y.-Z., Zheng, L., Lu, S. and Lin, Y.-T. 1996. Paralytic shellfish poisoning in southern China. *Toxicon* 34: 579-590.
- Binder, B. J. and Anderson, D. M. 1987. Physiological and environmental control of germination in *Scrippsiella trochoidea* (Dinophyceae) resting cysts. *J. Phycol.* 23: 99-107.
- Bolch, C. J. 2001. PCR protocol for genetic identification of dinoflagellates directly from single cysts and plankton cells. *Phycologia* 40: 162-167.
- Chang, D.-S., Shin, I.-S., Pyeun, J.-H. and Park, Y.-H. 1987. A study on paralytic shellfish poison of sea mussel, *Mytilus edulis*, Korea. *Bull. Kor. Fish. Soc.* 20: 293-299 (in Korean).
- Cho, E. S., Kim, C. S., Lee, S. G. and Chung, Y. K. 1999. Binding of alcian blue applied to harmful microalgae from Korean coastal waters. *Bull. Natl. Fish. Res. Dev. Inst.* 55: 133-138.
- Cho, H.-J. and Matsuoka, K. 2001. Distribution of dinoflagellate cysts in surface sediments from the Yellow Sea and East China Sea. *Mar. Micropaleontol.* 42: 103-123.
- Cho, H.-J., Matsuoka, K., Lee, J.-B. and Moon, C.-H. 2001. Dinoflagellate cyst assemblages in the surface sediments from the northwestern East China Sea. *J. Fish. Sci. Tech.* 4: 120-129.
- Cho, H.-J., Kim, C.-H., Moon, C.-H. and Matsuoka, K. 2003. Dinoflagellate cysts in Recent sediments from the southern coastal waters of Korea. *Bot. Mar.* 46: 332-337.
- Dale, B. 1976. Cyst formation, sedimentation, and preservation: factors affecting dinoflagellate assemblages in Recent sediments from Trondheimsfjord, Norway. *Rev. Palaeobot. Palynol.* 22: 39-60.
- Dale, B. 1983. Dinoflagellate resting cysts: "benthic plankton." In: *Survival Strategies of the*

- Algae*, Fryxell, G. A. (ed.). Cambridge University Press, Cambridge. pp. 69-136.
- Dale, B., Thorsen, T. A. and Fjellså, A. 1999. Dinoflagellate cysts as indicators of cultural eutrophication in the Oslofjord, Norway. *Estuar. Coastal Shelf Sci.* 48: 371-382.
- Dale, B., Dale, A. L. and Jansen, J. H. F. 2002. Dinoflagellate cysts as environmental indicators in surface sediments from the Congo deep-sea fan and adjacent regions. *Palaeogeogr. Palaeoclimat. Palaeoecol.* 185: 309-338.
- Godhe, A., Otta, S. K., Rehnstam-Holm, A. S., Karunasagar, I. and Karunasagar, I. 2001. Polymerase chain reaction (PCR) based detection of *Gymnodinium mikimotoi* and *Alexandrium minutum* in field samples from Southwest India. *Mar. Biotechnol.* 3: 152-162.
- Godhe A., Rehnstam-Holm, A., Karunasagar, I. and Karunasagar, I. 2002. PCR detection of dinoflagellate cysts in field sediment samples from tropic temperate environments. *Harmful Algae* 1, 361-373.
- Goodman, D. K. 1987. Dinoflagellate cysts in ancient and modern sediments. In: *The Biology of Dinoflagellates*, Taylor, F. J. R. (ed.). Blackwell Scientific Publications, Oxford. pp. 649-722.
- Guo, X., Ford, S. E. and Zhang, F. 1999. Molluscan aquaculture in China. *J. Shellfish Res.* 18: 19-31.
- Han, M.-S., Jeon, J.-K. and Kim, Y.-O. 1992. Occurrence of dinoflagellate *Alexandrium tamarense*, a causative organism of paralytic shellfish poisoning in Chinhae Bay, Korea. *J. Plankton Res.* 14: 1581-1592.
- Han, M.-S., Jeon, J.-K. and Yoon, Y.-H. 1993. Distribution and toxin profiles of *Alexandrium tamarense* (Lebour) Balech (dinoflagellate) in the southeastern coast waters. *Kor. J. Phycol.* 8: 7-13.
- Harland, R. 1983. Distribution maps of Recent dinoflagellate cysts in bottom sediments from the North Atlantic ocean and adjacent seas. *Palaeontology* 26: 321-387.
- Hyun, J.-H. and Kim, K.-H. 2003. Bacterial abundance and production during the unique spring phytoplankton bloom in the central Yellow Sea. *Mar. Ecol. Prog. Ser.* 252: 77-88.
- Jeon, J.-K., Yi, S. K. and Huh, H. T. 1988. Paralytic shellfish poisoning of bivalves in the Korean waters. *J. Oceanol. Soc. Kor.* 23: 123-129 (in Korean).

- Jin, J. H. and Chough, S. K. 1998. Partitioning of transgressive deposits in the southeastern Yellow Sea: a sequence stratigraphic interpretation. *Mar. Geol.* 149: 79-92.
- Kim, H. G. 1997. Recent harmful algal blooms and mitigation strategies in Korea. *Ocean Res.* 19: 185-192.
- Kim, K.-Y. and Kim, C.-H. 2004. A molecular phylogenetic study on Korean *Alexandrium catenella* and *A. tamarense* isolates (Dinophyceae) based on the partial LSU rDNA sequence data. *J. Kor. Soc. Oceanogr.* 39: 163-171.
- Kim, C.-H. and Shin, J.-B. 1997. Harmful and toxic red tide algal development and toxins production in Korean coastal waters. *Algae* 12: 269-276 (in Korean).
- Kim, G., Yang, H.-S. and Kodama, Y. 1998. Distributions of transition elements in the surface sediments of the Yellow Sea. *Continental Shelf Res.* 18: 1531-1542.
- Kim, H. G., Lee, S. G., An, K. H., Youn, S. H., Lee, P. Y., Lee, G. K., Cho, E. S., Kim, J. B., Choi, H. G. and Kim, P. J. 1997. Recent red tides in Korean coastal waters. *Nat. Fish. Res. & Dev. Insti.* 280 pp. (in Korean)
- Kim, C. S. Bae, H. M., Yun S. J., Cho, Y. C. and Kim, H. G. 2000. Ichthyotoxicity of a harmful dinoflagellate *Cochlodinium polykrikoides*: aspect of hematological responses of fish exposed to algal blooms. *Kor. J. Fish. Sci. Tech.* 3: 111-117
- Kim, H. G., Jung, C. S., Lim, W. A., Lee, C. G., Kim, S. Y., Yoon, S. H., Cho, Y. C. and Lee, S. G. 2001. The spatio-temporal progress of *Cochlodinium polykrikoides* blooms in the coastal waters of Korea. *J. Kor. Fish. Soc.* 34: 691-696 (in Korean).
- Kim, K.-Y., Yoshida, M., Fukuyo, Y. and Kim, C.-H. 2002. Morphological observation of *Alexandrium tamarense* (Lebour) Balech, *A. catenella* (Whedon et Kofoid) Balech and one related morphotype (Dinophyceae) in Korea. *Algae* 17: 11-19.
- Kim, S.-Y., Moon, C.-H. and Cho, H.-J. 2003. Relationship between dinoflagellate cyst distribution in surface sediments and phytoplankton assemblages from Gwangyang Bay, a southern coastal area of Korea. *The Sea, J. Kor. Soc. Oceanogr.* 8: 111-120 (in Korea).
- Kim, C.-H., Park, G.-H. and Kim, K.-Y. 2004a. Sensitive, accurate PCR assays for detecting harmful dinoflagellate *Cochlodinium polykrikoides* using a specific oligonucleotide primer set. *J. Fish. Sci. Tech.* 7: 122-129.
- Kin-Chung, H. 1998. Variations in the PSP contents of shellfish in Hong Kong and the

- eastern coast of South China Sea. *J. Shellfish Res.* 17: 1657-1666.
- Lee, J.-S. 1996. Bioactive components from red tide plankton, *Cochlodinium polykrikoides*. *J. Kor. Fish. Soc.* 29: 165-173.
- Lee, J.-S., Shin, I.-S., Kim, Y.-M. and Chang, D.-S. 1997. Paralytic shellfish toxins in the mussel, *Mytilus edulis*, caused the shellfish poisoning accident at Geoje, Korea, in 1996. *J. Kor. Fish. Soc.* 30: 158-160 (in Korean).
- Lee, J.-B., Kim, D. Y. and Lee, J. A. 1998. Community dynamics and distribution of dinoflagellates and their cysts in Masan-Chinhae Bay, Korea. *J. Fish. Sci. Tech.* 1: 283-292.
- Lee, C. K., Kim, H. C., Lee, S. G., Jung, C. S., Kim, H. G. and Lim, W. A. 2001. Abundance of harmful algae, *Cochlodinium polykrikoides*, *Gyrodinium impudicum* and *Gymnodinium catenatum* in the coastal area of south sea of Korea and their effects of temperature, salinity, irradiance and nutrient on the growth in culture. *J. Kor. Fish. Soc.* 34: 536-544. (in Korean)
- Matsuoka, K. 1999. Eutrophication process recorded in dinoflagellate cyst assemblages- a case of Yokohama Port, Tokyo Bay, Japan. *Sci. Total Environ.* 231: 17-35.
- Matsuoka, K. and Fukuyo, Y. 2000. *Technical Guide for Modern Dinoflagellate Cyst Study*. WESTPAC-HAB/WESTPAC/IOC.
- Matsuoka, K. and Fukuyo, Y. 2003. Taxonomy of cysts. In: *Manual on Harmful Marine Microalgae*, Hallegraeff, G. M., Anderson, D. M. and Cembella, A. D. (eds). UNESCO Publishing, Paris. pp. 563-592.
- McGillicuddy, D. J., Jr., Signell, R. P., Stock, C. A., Keafer, B. A., Keller, M. D., Hetland, R. D. and Anderson, D. M. 2003. A mechanism for offshore initiation of harmful algal blooms in the coastal Gulf of Maine. *J. Plankton Res.* 25: 1131-1138.
- Miller, P. E. and Scholin, C. A. 1996. Identification of cultured *Pseudo-nitzschia* (Bacillariophyceae) using species-specific LSU rRNA-targeted fluorescent probes. *J. Phycol.* 32: 646-655.
- Miserez, R., Pilloud, T., Cheng, X., Nicolet, J., Griot, C. and Frey, J. 1997. Development of a sensitive nested PCR method for the detection of *Mycoplasma mycoides*. *Mol. Cell. Probes* 11: 103-111.
- Naimie, C. E., Blain, C. A. and Lynch, D. R. 2001. Seasonal mean circulation in the Yellow

- Sea- a model-generated climatology. *Continental Shelf Res.* 21: 667-695.
- Nunn, G. B., Theisen, B. F., Christensen, B. and Arctander, P. 1996. Simplicity-correlated size growth of the nuclear 28S ribosomal RNA D3 expansion segment in the crustacean order Isopoda. *J. Mol. Evol.* 42: 211-223.
- Park, Y. A. and Khim, B. K. 1992. Origin and dispersal of recent clay minerals in the Yellow Sea. *Mar. Geol.* 104: 205-213.
- Park, J. S. and Yoon, Y. H. 2003. Marine environmental characteristics by distribution of dinoflagellates cysts in the southwestern coastal waters of Korea - 1. Spatio-temporal distribution of dinoflagellates cysts in Gamak Bay. *J. Kor. Fish. Soc.* 36: 151-156 (in Korean).
- Park, G.-H., Kim, K.-Y, Kim, C.-H. and Kim, H. G. 2004a. Spatio-temporal distribution of dinoflagellate resting cysts at the Saemangeum area. *J. Kor. Fish. Soc.* 37: 202-208 (in Korean).
- Park, T.-G., Kim, C.-H. and Oshima, Y. 2004b. Paralytic shellfish toxin profiles of different geographic populations of *Gymnodinium catenatum* (Dinophyceae) in Korean coastal waters. *Phycol. Res.* 52: 300-305.
- Pfiester, L. A. and Anderson, D. M. 1987. Dinoflagellate reproduction. In: *The Biology of Dinoflagellates*, Taylor, F. J. R. (ed.). Blackwell Scientific Publications, Oxford. pp. 611-648.
- Sætre, M. M., Dale, B., Abdullah, M. I. and Sætre, G.-P. 1997. Dinoflagellate cysts as potential indicators of industrial pollution in a Norwegian Fjord. *Mar. Environ. Res.* 44: 167-189.
- Saito, K., Drgon, T., Robledo, J. A. F., Krupatkina, D. N. and Vasta, G. R. 2002. Characterization of the rRNA locus of *Pfiesteria piscicida* and development of standard and quantitative PCR-based detection assays targeted to the nontranscribed spacer. *Appl. Environ. Microbiol.* 68: 5394-5407.
- Sako, Y., Hosoi-Tanabe, S. and Uchida, A. 2004. Fluorescence in situ hybridization using rRNA-targeted probes for simple and rapid identification of the toxic dinoflagellates *Alexandrium tamarense* and *Alexandrium catenella*. *J. Phycol.* 40: 598-605.
- Scholin, C., Miller, P., Buck, K., Chavez, F., Harris, P., Haydock, P. and Howard, J. 1997. Detection and quantification of *Pseudo-nitzschia australis* in cultured and natural

- populations using LSU rRNA-targeted probes. *Limnol. Oceanogr.* 42: 1265-1272.
- Sharrock, A. D. 1994. The design of primers for PCR. In: *PCR Technology: Current Innovations*, Griffin, H. G. and Griffin, A. M. (eds). CRC Press, Boca Raton. pp. 5-11.
- Shi, X., Chen, Z., Cheng, Z., Cai, D., Bu, W., Wang, K., Wei, J. and Yi, H.-I. 2004. Transportation and deposition of modern sediments in the southern Yellow Sea. *J. Kor. Soc. Oceanogr.* 39: 57-71.
- Suh, Y. S., Jang, L.-H., Lee, N.-K. and Ishizaka, J. 2004. Feasibility of red tide detection around Korean waters using satellite remote sensing. *J. Fish. Sci. Tech.* 7: 148-162.
- Tengs, T., Bowers, H. A., Ziman, A. P., Stoecker, D. K. and Oldach, D. W. 2001. Genetic polymorphism in *Gymnodinium galatheanum* chloroplast DNA sequences and development of a molecular detection assay. *Mol. Ecol.*, 10, 515-523.
- Turgeon, J., Cembella, A. D., Therriault, J.-C. and Beland, P. 1990. Spatial distribution of resting cysts of *Alexandrium* spp. in sediments of the lower St. Lawrence estuary and the Gaspé coast (eastern Canada). In: *Toxic Marine Phytoplankton*, Granéli, F., Sundström, B., Edler, L. and Anderson, D. M. (eds). Elsevier, New York. pp. 238-243.
- Tyler, M. A., Coats, D. and Anderson, D. M. 1982. Encystment in a dynamic environment: deposition of dinoflagellate cysts by a frontal convergence. *Mar. Ecol. Prog. Ser.* 7: 163-178.
- Tyrrell, J. V., Connell, L. B. and Scholin, C. A. 2002. Monitoring for *Heterosigma akashiwo* using a sandwich hybridization assay. *Harmful Algae* 1: 205-214.
- Uehara, K. and Saito, Y. 2003. Late Quaternary evolution of the Yellow/East China Sea tidal regime and its impacts on sediments dispersal and seafloor morphology. *Sediment. Geol.* 162: 25-38.
- Versteegh, G. J. M. 1994. Recognition of cyclic and non-cyclic environmental changes in the Mediterranean Pliocene: a palynological approach. *Mar. Micropaleontol.* 23: 147-183.
- Wall, D., Dale, B., Lohmann, G. P. and Smith, W. K. 1977. The environmental and climatic distribution of dinoflagellate cysts in modern marine sediments from regions in the North and South Atlantic Oceans and adjacent seas. *Mar. Micropaleontol.* 2: 121-200.
- Wang, Z., Matsuoka, K., Qi, Y. and Chen, J. 2004. Dinoflagellate cysts in Recent sediments from Chinese coastal waters. *Mar. Ecol.* 25: 289-311.

- White, A. W. and Lewis, C. M. 1982. Resting cysts of the toxic, red tide dinoflagellate *Gonyaulax excavata* in Bay of Fundy sediments. *Can. J. Fish. Aquat. Sci.* 39: 1185-1194.
- Yamaguchi, M., Itakura, S., Imai, I. and Ishida, Y. 1995. A rapid and precise technique for enumeration of resting cysts of *Alexandrium* spp. (Dinophyceae) in natural sediment. *Phycologia* 34: 207-214.
- Yoshida, M., Mizushima, K., Matsuoka, K. 2003. *Alexandrium acatenella* (Gonyaulacales: Dinophyceae): Morphological characteristics of vegetative cell and resting cyst. *Plankton Biol. Ecol.* 50: 61-64.
- Zhou, M., Li, J., Luckas, B., Yu, R., Yan, T., Hummert, C. and Kastrup, S. 1999. A recent shellfish toxin investigation in China. *Mar. Pollut. Bull.* 39: 331-334.

Summary (in Korean)

황해 저질 내 외편모조류 휴면포자 분포와 PCR 기법을 이용한 유해적조 생물 검출

황 철 희

부경대학교 대학원 수산생물학과

요 약

황해 내 존재하는 외편모조류 휴면포자의 분포를 파악하기 위하여 총 33개의 저질 시료를 고생물학적인 방법으로 처리, 분석하였다. 채집 지역은 산둥 반도와 제주도 사이이며 4개의 latitudinal transect로 이루어졌다. 각각의 transect는 6-9개의 정점으로 이루어졌으며 한국과 중국을 잇고 있다. 전체적으로 26 종류의 휴면포자가 관찰되었으며, *Gonyaulax scrippsae*, *Alexandrium* spp. (타원형) 및 *G. spinifera*가 주요 우점종으로 나타났다. 4개의 transect를 대상으로 바깥쪽의 2 transect보다는 안쪽의 2 transect에서 휴면포자의 높은 밀도를 관찰할 수 있었다. 각 transect내에서는 황해 중심해역에서 높은 밀도를 나타내었으나, 한국과 중국의 각 연안쪽에 가까울수록 그 밀도가 감소하였다. 이러한 경향은 황해 내 조류의 움직임, 저질의 형상 및 수심과 같은 수로학적 특성과 연관이 깊은

것으로 사료된다.

한편, 한국 연안에서는 *Alexandrium tamarense*와 *Cochlodinium polykrikoides*와 같은 유해 와편모조류의 발생 증가에 의해 막대한 수산 피해를 받고 있다. 따라서 저질 내에 존재하는 휴면포자를 대상으로 종 특이적 primer 쌍을 이용한 PCR증폭 실험을 실시하였으며, 이를 유해적조 모니터링에의 이용성에 대해 검토해 보았다. 먼저 육상에 존재하는 황토와 해양의 저질에서 bulk DNA를 추출하여 실험하였다. 황토에서의 PCR증폭은 음성 반응을 보였으나 인위적으로 타원 형태의 *Alexandrium* spp. 의 휴면포자를 첨가한 황토에서는 양성 반응을 나타냄으로써, 육상의 황토를 해양 저질에 대한 음성 대조구로 사용할 수 있는 것으로 확인되었다. 특히, 황해의 저질을 이용한 실험에서는 *A. tamarense*와 *C. polykrikoides*의 종 특이적 primer쌍에 의해 양성 반응을 나타내었다. 또한 PCR과정 중 annealing temperature가 비특이적인 반응 결과에 연관되는 것을 확인할 수 있었다. 이 문제는 annealing temperature를 상승시킴으로써 해결할 수 있었다. 한편, *C. polykrikoides* 검출 실험에서는 저질 내 대상종의 밀도를 산정하기 힘든 관계로 nested PCR을 실시한 결과, 저질 중에 이 종이 명확히 존재하는 것이 확인되었다. 따라서 이러한 분자생물학적 검출기술을 바탕으로 생활사가 완전히 해명되지 않은 *C. polykrikoides*와 같은 유해종의 존재 여부를 판단하고 지역적 모니터링에 활용할 수 있을 것으로 기대된다.

Acknowledgements

I wish to express my gratitude to my supervisor, Prof. Chang-Hoon Kim, giving me the opportunity to study and invaluable advice. I am also much indebted to Prof. Yoon Kwon Nam and Jong-Myung Kim in Pukyong National University. I would like to thank Dr. Keun-Yong Kim for his useful comment, valuable discussion and for critical reading of a part of the manuscript.

Special tanks are due to Dr. Seung Heo and Dr. Yoon Lee of NFRDI for their valuable comments on this study. I would like to acknowledge members of Lab. of Aquaculture & the Environment (Dr. Young-Soo Kim, Gi-Hong Park, Shin-Hong Ahn, Yoo-Hong Min, Sung-Wook Jang, In-Joo Kim, So-Eun Cho, Jae-Wook Ahn, Ji-Young Kang, Jung-Kyung Park, Ho-Jung Ha, Suck-Ki Kim, Kook-Il Lee, Mi-Kyung Kim and Mi-Young Kim). I also would like to thank Seung-Jin Ha, Hyun-Sick Kim in Fisheries Science & Technology Center of PKNNU and Myung-Baek Shon in Marine Eco-Technology Institute. I also thank to Jae-Beom Shin and Hak-Chul Lee.

Finally, I must express my sincere thanks to my family for their constant supports to me.